W. BEN MABROUK
J. BELHADJ
M. PIETRZAK-DAVID

J. Electrical Systems x-x (2010): x-xx

5.1. Regular paper

Electromechanical Multi-machine System for Railway

Modelling, Analysis and Control

The authors develop an electrochemical multi-machine system for railway traction application. The train bogie system constituted of two induction motors (IM), fed by one voltage source inverter (VSI) is studied. It is piloted by a Mean Rotor Field Oriented Control (MRFOC). This system has a depending operation amplified by strong electric, magnetic and mechanical couplings. This study is focused on the mechanical coupling between a common load of the both motors carried out by two mechanical transmissions and two rail-wheel contacts. So, this bogie system is a high order non-linear one. Different simulations are presented and discussed in balanced and unbalanced system operation conditions.

Keywords: Railway traction, Parallel Induction Drive, Mechanical Transmission, Adherence coefficient, Multi-machine Multi-inverter, Mean control.

1. Nomenclature

P	Pairs of poles number
M_{sr}	Cyclic mutual induction
L_r	Cyclic rotor inductance
J_3 (I_3)	Principal gear wheel inertia
J_4 (I_4)	Intermediate gear wheel inertia
J_5 (I_5)	Driving pinion inertia
J_6 (I_6)	Rotor inertia
J_9 (I_9)	plate fixed on the axle inertia
K_{acc}	Mechanical coupling Stiffness
c_{acc}	Mechanical coupling flexibility
K_4	Stiffness of teeth enters pinions 4 and 3
K_5	Stiffness of teeth enters pinions 4 and 5
K_{jac}	Jacquemin transmission stiffness
c_{jac}	Jacquemin transmission flexibility
K_{ess}	Axle torsion stiffness
R_3	Principal gear wheel radius
R_4	Intermediate gear radius
R_5	Motor pinion radius
R_{wheel}	Wheel radius
J_{wheel}	Wheel inertia
M_{train}	Mass train

Induction motor parameters
Pole pairs: 2
Motor speed: 4160 tr/min
Stator resistance: 29.4 mΩ
Rotor resistance: 25.5 mΩ

Mutual inductance: 18.6 mH
Stator inductance: 19.272 mH
Rotor inductance: 19.244 mH

2. Introduction

Electric railway traction systems are complex and have different strong electric, magnetic and mechanical coupling. These couplings impose several constraints which complicate the modelling and analysis of these systems. Multi-machine/Multi-inverter System (MMS) well used in order to satisfy the industrial requirements such as the optimization of the system volume and weight. Many configurations are developed and analyzed to guarantee operation stability when a mechanical or electrical disturbance appears [1-3]. The studied system, called BO-BO, is composed of two induction motors IM; each bogie motor has four driving wheels driven by two induction motors [4]. So, one inverter is often applied to feed connected in parallel induction motors. We consider that both motors have the same parameters and consequently the same behaviour. A mean FOC control is chosen to drive

Corresponding author : W.BEN MABROUK
Unité de recherche LSE, Ecole Nationale d'Ingénieurs de Tunis (ENIT), Tunis – Tunisia
bmwiem2002@yahoo.fr,

each IM; this structure is interesting due to their coast and size [5-6].
In this study, we will interest particularly on the modelling and analysis of mechanical interaction. This one is composed of mechanical transmission coupling to each motor; it reduces the motor speed transmitting to the wheel. A contact wheel-rail creates the force allowing the advance of the train, the transmitted force to the rail is limited by a variation of adherence coefficient. In fact, when an adherence loss is produced, the wheel is slipping and it creates perturbations to all the system, especially in the electric part.
Firstly, a description of studied system is presented. Then, the load mechanical coupling is modelled therefore an analytical model is given. Finally, precise simulations are made to illustrate the dynamics of the railway traction system in adherence loss conditions.

3. Presentation of studied system

Railway traction system studied in this paper is composed of two bogies moved by four 3-phases induction motors especially designed and optimized for traction. Each "two motors" is devices fed by 3-leg voltage source inverter (VSI) connected to the catenaries (25KV-50Hz) through the pantograph [4]. The bogie ensures a two motor mechanical coupling through a locomotive chassis. In this study a description of one bogie is presented and analyzed, and its structure is shown in Fig .1.
The DC voltage E is obtained from the catenaries via a rectifier and an RLC input filter. Different structures depending of catenaries are presented and compared in [4]. The MMS structure envisaged is mono-inverter bi-motor when a single inverter feeds the both motors. This inverter is driven by a mean RFOC control [5-8]. The control inputs are obtained by a calculation of different variables of two motors (current, speed); in this case we can optimize the number of applied sensors. When the average value motors are identical mechanical transmission which provides a traction force transmitted to the wheels through the wheel- rail contact. Both wheels are coupled through locomotive chassis; this coupling can introduce system instability when a loss adherence or loss contact of the pantograph catenaries is produces. The authors formulate an exact mathematical model taking into account the mechanical coupling.

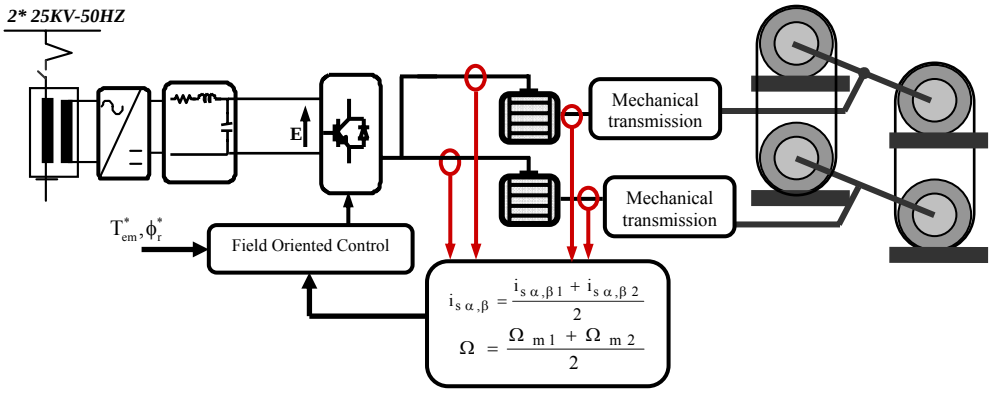

Fig.1: Studied railway traction system, drive system with two parallel connected induction motors

4. Multi-machines multi-inverter system

Multi-Machines Multi-Inverters System (MMS) are recently developed for many industrials applications which some machines are driven by some inverters. This class of system offers

a reduction of design time, the cost and the optimization of the volume of embarked systems.
In this study, the global system is composed of four induction motors therefore many configurations are possible. The first is to drive each motor (IM) by own inverter, this structure is used in several industrial applications with a good operating stability. However, it makes a duplication of components. The second configuration is to drive all IM by one inverter. This structure is interested cost, optimisation components and volume but it presents strong electric coupling in the common inverter and mechanical coupling in the coupled loads. The third proposed configuration is mono-inverter / bi-motors that two IM are fed by one inverter. This structure offers optimisation components and volume and also it has strong electric coupling through a common inverter.

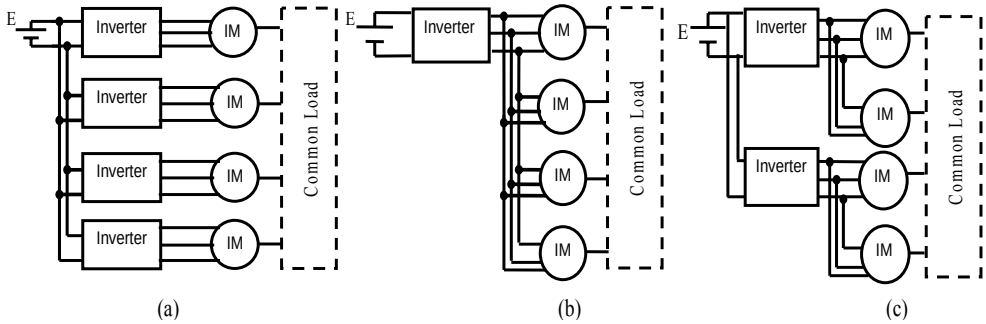

Fig.2: Different Muli-Machine Multi-Inverter configurations

The volume and weight optimizations, the reliable operations with small maintenance service and also not expansive cost of these embedded systems formulate the main concept arguments of choice of mono inverter / bi motors system. In traction railway system, mono-inverter / bi-motors offers a good stability often in undisturbed functioning and tries to maintain higher performances in disturbed functioning. These induction motors (IM) are designed for traction application

5. Modelling of mechanical load of traction system

The Mechanical part of railway traction system is a complex part which constituted of two mechanical transmissions, a rail- wheel contact and a common case dynamics, it shows in Fig.3. The mechanical transmission connects the induction motors to the wheel and reduced the mechanical speed with gear ratio of the 3 plats of reducer. The rail –wheel contact consist to convert the rotational speed on linear speed. However, this contact is not punctual and it depends of adherence coefficient which provides the advanced force. The case dynamics determine different efforts supported by each wheel.

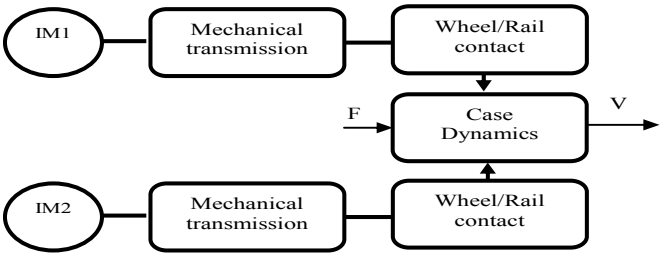

Fig.3: General Diagram of mechanical load

5.1. Mechanical transmission part

Fig.2 represents the general diagram of the mechanical transmission composed of the motor inertia fixed by a first coupling element followed by a reducer with three plates. In its output another coupling element is present before wheel inertia [9-10].

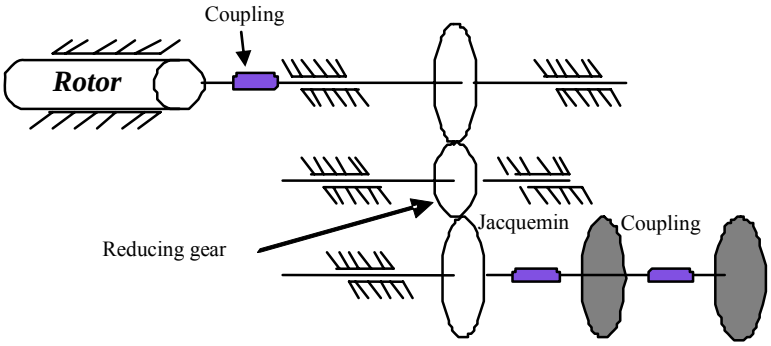

Fig.4: Synoptic scheme of the mechanical transmission

In order to establish the mathematical model of the mechanical transmission, the Bond Graph model is applied. This Bond Graph is given by ALSTHOM industrial [10-11]; we formulate and deduce the mathematical equation of mechanical transmission line. A various elements in fig.3 are characterized by inertia flexibility and stiffness (I, R, C) presented. Different studies show that the mechanical resonance frequency is around 18HZ [6, 10].

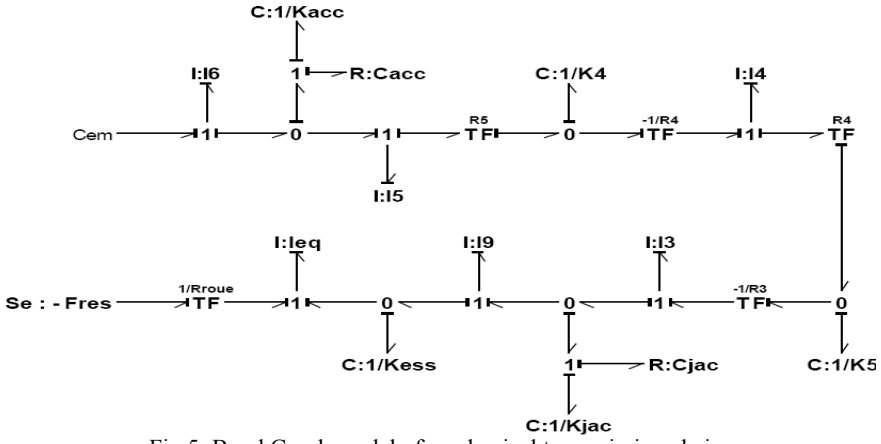

Fig.5: Bond Graph model of mechanical transmission chain

From this Bond Graph model, an analytical model is developed and it presents as a 10 order state equation, Eq.(1). This model is non linear and depends of various mechanical parameters, it allows to determinate mechanical variables transmitted on the wheel. The advanced force is created by the contact between wheel and rail, this contact is assumed to be in a single point but practically it is a surface contact representing by experimental adhesion coefficient. In the aim to simplify the study, many works is limited to contact without slip, by neglecting the effect of Wheel-Rail contact [8, 11]. This complex method represents a physical phenomenon which must be studied for modelling of the mechanical load. Consequently we obtain the system equations as below.

$$\begin{cases} \dfrac{dC_{Acc}}{dt} = Kacc(\Omega_m - \Omega_{Acc}) \\ \dfrac{d\Omega_{acc}}{dt} = \dfrac{C_{Acc} + c_{acc}.(\Omega_m - \Omega_{Acc}) - C_1}{J_5} \\ \dfrac{dC_1}{dt} = R_5.K_4.(R_5.\Omega_{Acc} + R_4.\Omega_1) \\ \dfrac{d\Omega_1}{dt} = -\dfrac{R_4.(\dfrac{C_1}{R_5} - \dfrac{C_{red}}{R_3})}{J_4} \\ \dfrac{dC_{red}}{dt} = -R_3.K_5.(R_4.\Omega_1 + R_3.\Omega_{red}) \\ \dfrac{d\Omega_{red}}{dt} = \dfrac{C_{red} - c_{jac}.(\Omega_{red} - \Omega_{ess}) - C_{ess}}{J_3} \\ \dfrac{dC_{ess}}{dt} = K_{jac}.(\Omega_{red} - \Omega_{ess}) \\ \dfrac{d\Omega_{ess}}{dt} = \dfrac{c_{jac}.(\Omega_{red} - \Omega_{ess}) + C_{ess} - C_{wheel}}{J_9} \\ \dfrac{dC_{wheel}}{dt} = K_{ess}.(\Omega_{ess} - \Omega_{wheel}) \\ \dfrac{d\Omega_{wheel}}{dt} = \dfrac{C_{wheel} - .C_R}{J_{Wheel}} \end{cases} \quad (1)$$

Where:
(C_{red},Ω_{red}) are the torque and speed of the outside reducer.
(C_{ess}, Ω_{ess}) are the torque and speed of outside axle.
(C_{Acc}, Ω_{Acc}) are the torque and speed of outside coupling.
(C_1, Ω_1) are the torqe and speed of intermediate gear.
(C_{wheel}, Ω_{wheel}) are the torque and speed of wheel.
C_R is the torque created by the traction force. It is defined by the following equation:

$$C_R = F_{\_av} . R_{wheel} \quad (2)$$

Another equation is to present the torque of electric motor governed by Eq.(3), where C_L is the load torque of induction motor corresponding to the tangential force between driving wheel and rail which is shown in Eq.(4).

$$J_6 . \frac{d\Omega_m}{dt} = C_{em} - C_L \quad (3)$$

$$C_L = F_{\_av} . R_{wheel} . \frac{R_5}{R_3} \quad (4)$$

5.2. Wheel- Rail contact

The transmitted force is the result of the contact between wheel and rail; it is characterized by a very low adherence coefficient (μ) which limits the maximal value of effort [9, 12-13]. In fact, the maximal coefficient (μ_{max}), called adhesion coefficient, is strongly affected by

the rails and driving wheels condition. It decreases when the train has a slip phenomenon and, consequently, the totality effort is not transmitted. Adherence between wheel and rail is a very important function to maintain safety and stable operation from the standpoint of braking and driving, in particular under wet conditions at the rail-wheel interface [11-13]. This coefficient has an experimental value depending also of gauge and mass of train; it will have a variation according to the absolute slip velocity (v_S) as shown in Fig.6.

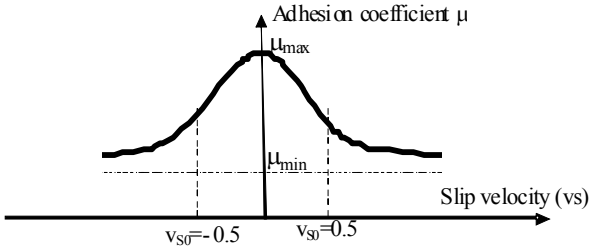

Fig.6: Characteristics between adhesion μ and slip velocity

The value of μ is not constant, it can assume different value for the same wheel-rail system and it depends of state of rail of which generate a slipping phenomenon represented by Eq.(5).

$$v_S = \frac{V - R_{wheel}.\Omega_{wheel}}{|V|} \tag{5}$$

The following equation represents the analytic function of μ deduced by Fig.6.

$$\begin{aligned} &\text{if } v_S \geq v_{S0} \text{ than} \\ &\mu = -aa.(1 - \exp(-10.(|v_S| - v_{S0}))) + bb \\ &\text{else} \\ &\mu = aa.(1 - \exp(10.(|v_S| - v_{S0}))) + bb \end{aligned} \tag{6}$$

Where: $aa = \frac{\mu_{max} - \mu_{min}}{2}$ and $bb = \frac{\mu_{max} + \mu_{min}}{2}$

$v_{S0} = 0.5$ is the limit value of slipping.

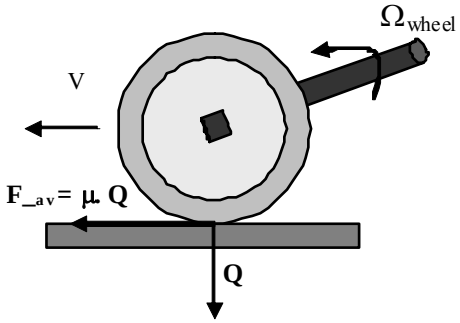

Fig.7: Driven wheel representation

The transmitted effort $F_{\_av}$ is described in general by the following equation:

$$F_{\_av} = \mu . Q \tag{7}$$

Q is the weight of locomotive supported by wheel, it is a radial force. It calculated by considering the dynamic case [8, 11]. The transmitted effort may be increased by maximising the adhesion coefficient whose corresponds to a small value of slip velocity. The value of μ is not constant, it can assume different values for the same wheel-rail system and it depends of rail state and can generate a slipping phenomenon.

5.3. Case dynamics

Electric train moves by the tangential force between its driving wheel and the rail. Fig.8 shows the structure of mi-bogie. Using the fundamental dynamic principle applied to bogie and case [5, 11-13] we calculate different efforts supported by each wheel. .

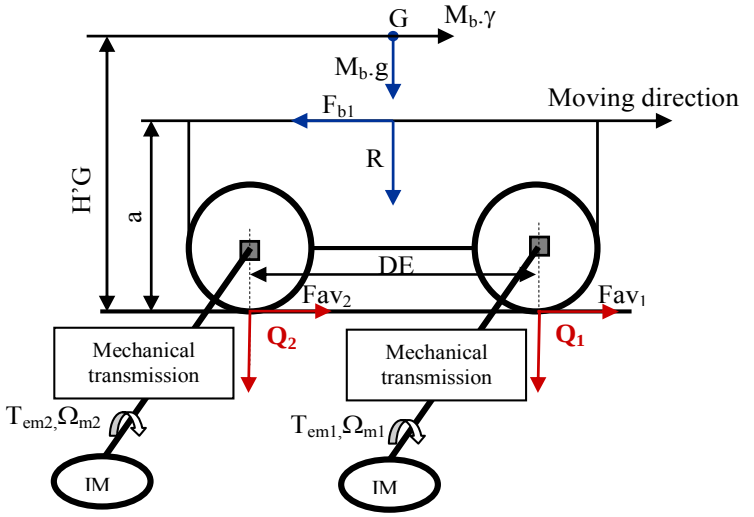

Fig.8: Representation of mi-bogie

Q_1 and Q_2 are calculated by the following equations:

$$\begin{cases} Q_1 = \frac{1}{2}.(M_b.g + \frac{M_C.g}{2} - \frac{F.(H-a) + M_C.\gamma.(HG-a)}{DB}) - \frac{M_b.\gamma.(HG-a) + (F_{\_av1} + F_{\_av2}).a}{DE} \\ Q_2 = \frac{1}{2}.(M_b.g + \frac{M_C.g}{2} - \frac{F.(H-a) + M_C.\gamma.(HG-a)}{DB}) + \frac{M_b.\gamma.(HG-a) + (F_{\_av1} + F_{\_av2}).a}{DE} \end{cases} \tag{8}$$

These expressions depend of mass, distances between wheel, bogie and case; also it depends of advanced forces and resistive force F. The resistance force F can be approximated by the following equation, Eq.(9), where the coefficient "A" models static friction, "B" accounts for dynamic friction and "C" denotes aerodynamic resistance [6]. The values of these coefficients take account of factors arising from the train.

$$F(N) = A + B.V + C.V^2 \tag{9}$$

V is the linear velocity of train, (m/s)
The acceleration achievable depends on the transmitted effort available and the train mass. So, a linear velocity of train is calculated by integrate the following equation:

$$F_{\_av1} + F_{\_av2} - F = M_{train} \cdot \frac{dV}{dt} \tag{10}$$

6. Drive control structures

The digital control strategy offer to mono/inverter bi/motors system is Mean Rotor Filed Oriented Control MRFOC that the reference control inputs are obtained by average of different signals of both motors (current, speed) [1, 5-8]. Rotor Field Oriented Control is one of the best method to drive IM and presents a satisfactory performances for traction applications [1-2]. It requires that the rotor flux φ_r and electromagnetic torque T_{em} have to be decoupled. For the IM modelling, done in (d, q) reference frame, with "d" axis linked with the rotor flux vector. The rotor flux and electromagnetic torque expressions can be written as follows.

$$\varphi_r = \varphi_{rd} \tag{11}$$

$$T_{em} = P.\frac{M_{sr}}{L_r}\varphi_{rd} \cdot i_{sq} \tag{12}$$

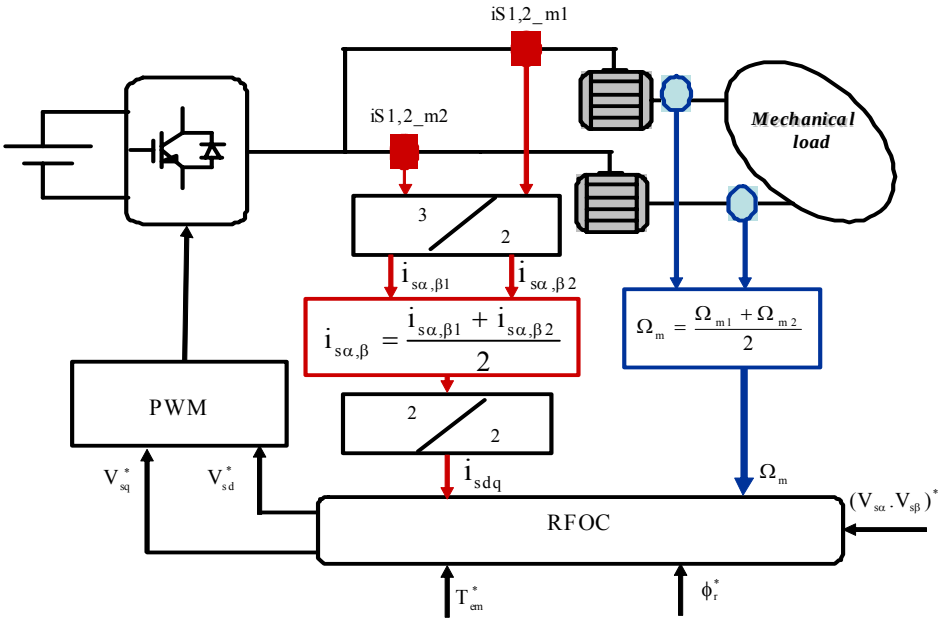

Fig.9: Mean control (MRFOC) scheme

Mean control strategy considers the average of the different input variables of both IM to create "virtual mean motor". The measured variables of both motors are the currents ($i_{s\alpha\beta1}$, $i_{s\alpha\beta2}$) and the speed (Ω_{m1}, Ω_{m2}). The average variables are obtained using equations Eq.(13) and Eq.(14).

$$i_{s\alpha,\beta} = \frac{i_{s\alpha,\beta 1} + i_{s\alpha,\beta 2}}{2} \tag{13}$$

$$\Omega = \frac{\Omega_{m1} + \Omega_{m2}}{2} \tag{14}$$

Mean RFOC control offers symmetric behaviours of both motors to obtain stable average performance. On undisturbed functioning, both motors are identical so they have the same behaviours. However, when a disturbance affects one motor the second reacts to it compensate, so it is also disturbed. The mean control reacts to offer a stable average signals.

7. Simulation results

Several numerical simulations have been carried out in order to validate the structure of railway traction system in normal and perturbation mode. In Fig.10 mechanical Reponses corresponding to balanced functioning is presented. We observe that the wheel speed has a same behaviour than mechanical motor speed with a reduced value; this value corresponds to the gear ratio. Also, the induction motor torque increase with the same gear ratio and it presents some oscillation at starting. These oscillations are the result of mechanical inertias and stiffness.

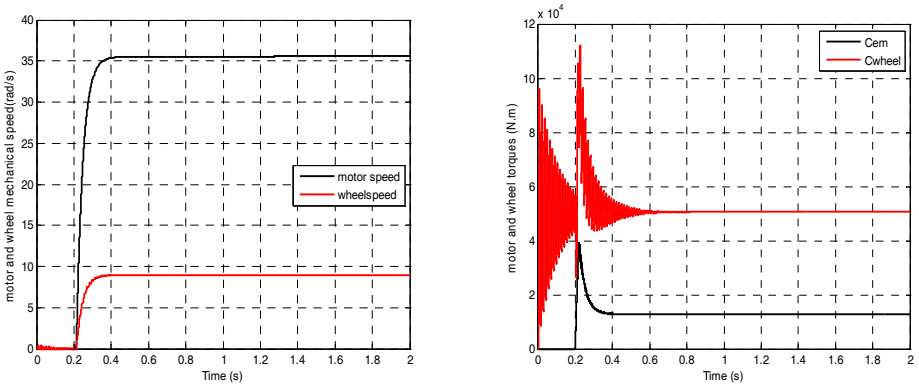

Fig.10: Mechanical variable responses

The most mechanical problems for railway traction system are the adherence loss of wheels. This phenomenon generates a very strong variation in the system performances because the two motors see a different load torque. Consequently, their behaviour will not be the same. A disturbed operation mode obtained by decreasing of adherence coefficient of one wheel. It generates a slip phenomenon of the driving wheel and modifies a linear train speed. In our simulation this phenomenon is introduced to second motor at 0.6s and takes place at 1.6s by a brutal fall of the maximum adherence coefficient (μ_{max}).

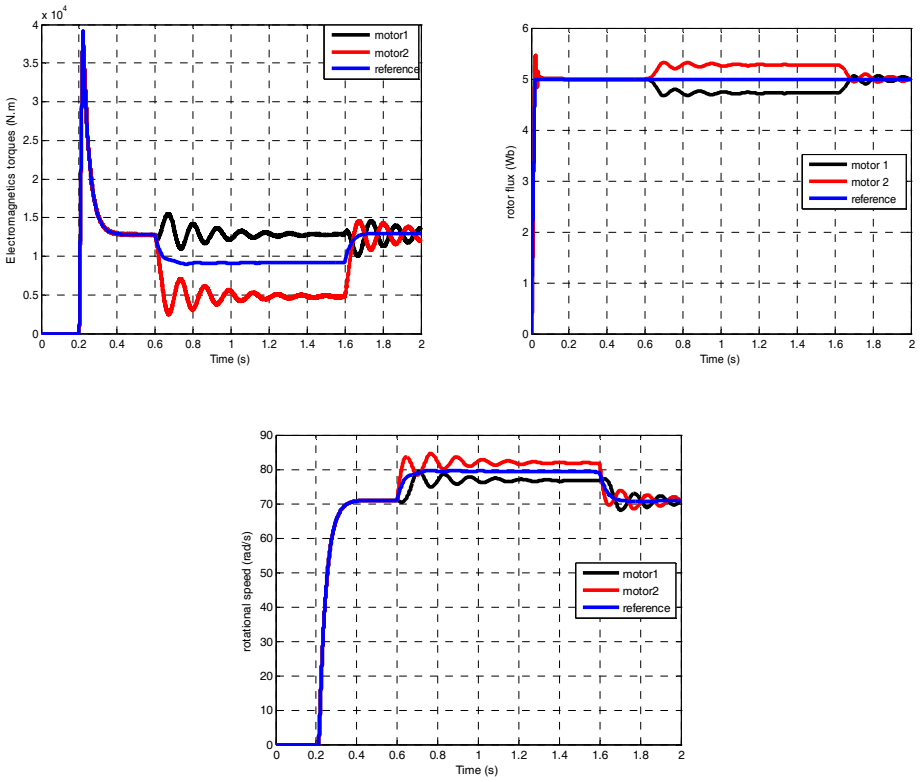

Fig.11: Electromagnetic torques, rotor fluxes and rotational speeds of both motors controlled by MRFOC

Fig.11 presents the electrical variables of both motors in the presence of system mechanical disequilibrium such as a loss adherence. This mechanical disturbance affects also the electric part and modifies the operation of each motor. When a disturbance acts on one IM, the second IM is also affected by it. Some oscillations occur in all variables of the system and the MRFOC strategy offers symmetric behaviours of both motors. Hence, we obtain stable average performances different in comparison with nominal motor performances. Also, we notice that the rotor flux and the rotational speed of the motor 1 increase, meanwhile motor 2 tries to compensate this augmentation in order to maintain the mean variables equal to their reference. The torque of motor 2 decreases so motor 1 tries to compensate this reduction.

These variations of induction motor performances are consequently seen on mechanical part. The perturbation is the same produced by lost of adherence coefficient as Fig.12 and Fig.13. These figures show the different mechanical speed (Ω_{wheel}) and torque (T_{wheel}) transmitted on the wheel through mechanical transmission line. We observe some strong oscillations at coupled loads; they will be reduced after used the reducer and Jacquemin.

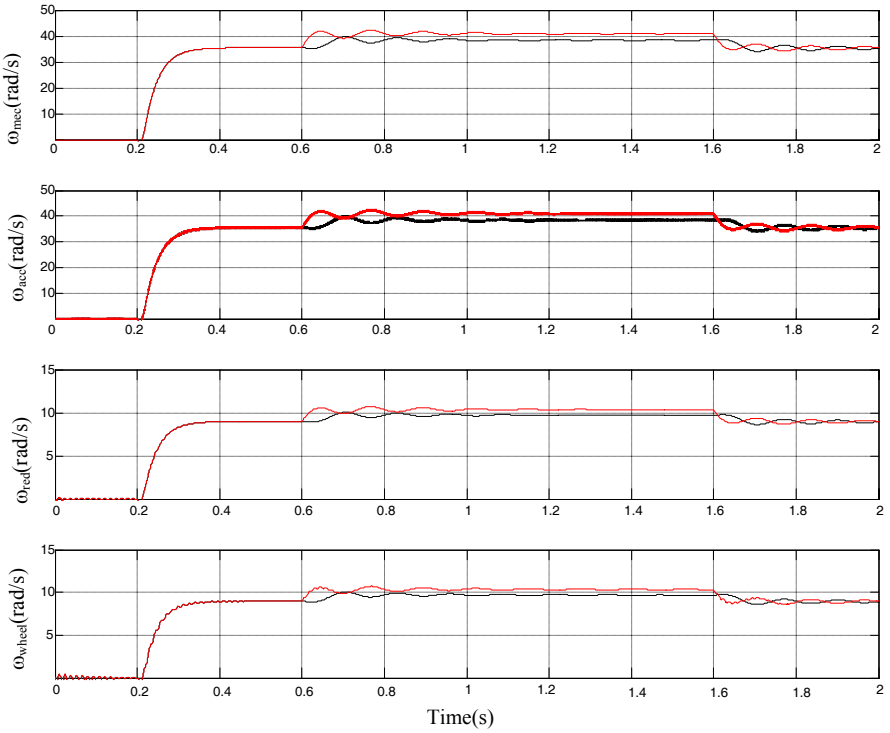

Fig.12: Different mechanical speeds of mechanical transmission in presence of lost of adherence

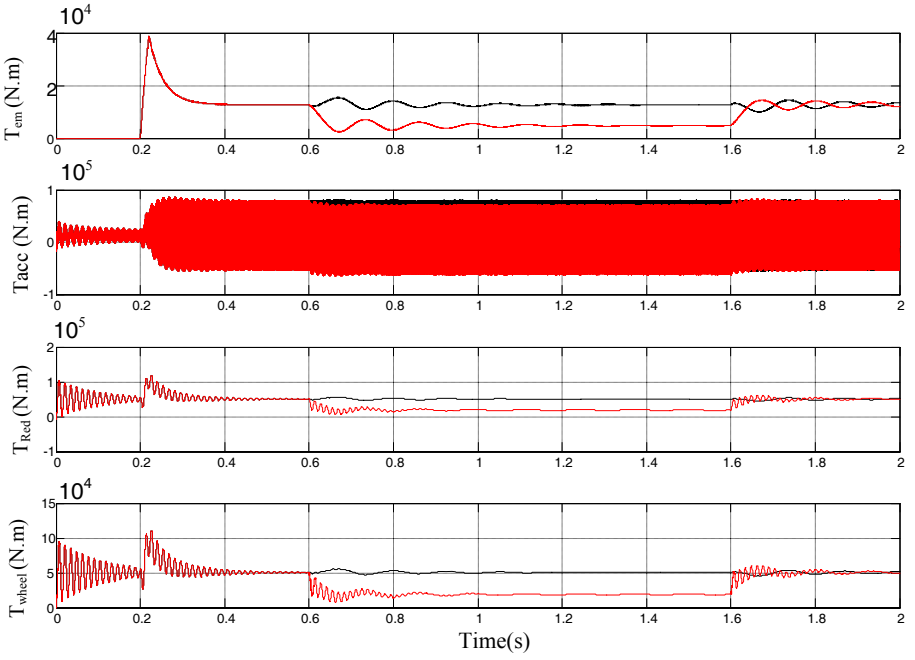

Fig.13: Different torques of mechanical transmission in presence of lost of adherence

The linear speed is shown on Fig.14. A few variations appear at 0.6s to 1.6s but train moving still accelerates.

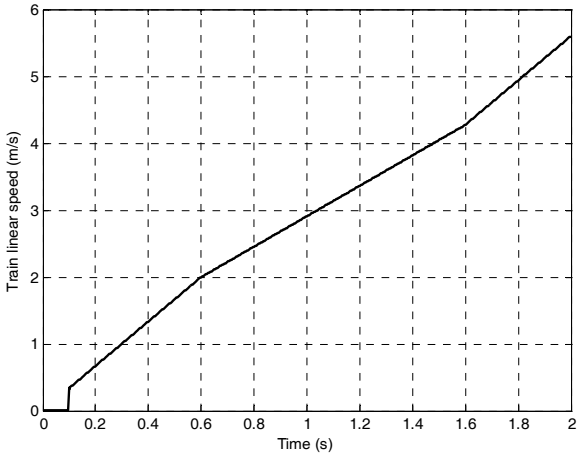

Fig.14: Evolution of the train linear speed

8. Conclusion

The authors give the modelling of the asynchrounes railway traction system with Mean Rotor Field Oriented Control (MRFOC), the study system including of Multi machine Multi inverter System where one inverter fed two induction motors. The MRFOC offers symmetric behaviours to both motors to guarantee a stable reference and good performances of all system even undisturbed functioning. Inductions motors are strongly coupled through mechanical load which presents a complex and a non linearity part. A development and analysis of mechanical load coupling are discussed in normal and unbalanced functioning. Some results are presented illustrate the mean control strategy performances applied to railway traction system.

References

[1] J. Belhadj "Modelling, Control and Analyze of Multi-Machine Drive Systems using Bond Graph Technique" Journal Electrical Systems 2-1, pp. 29-51, 2006

[2] P. Escané, C.Lochot, M. Pietrzak-David and B. de Fornel, "Electromechanical interactions in a high speed railway traction system", Electrimacs '99, Lisbon, Portugal,September 1999

[3] Internal report: "Projet d'électrification de La Banlieue Sud De Tunis UABT / DPBT / No.01/2006"

[4] M.M. Bakran, H.G. Eckel, P.Eckert, H.Gambach, U. Wenkemann "Comparison of multi-system traction converters for high power locomotives" in IEEE Power Electronics Specialists' Conference, PESC'2004, Achen, Germany, 2004

[5] W. Ben Mabrouk, J. Belhadj, M. Pietrzak-David, "Modelling and Control of electromechanical Multi machine System for Railway Traction", 2nd International conference on Electrical Engineering Design and Technologies, ICEEDT, 8-10, 2008, Hammamet Tunisia.

[6] R. Kaller and J.-M. Allenbach, Traction électrique, vol. 1, Presse Polytechniques et Universitaires Romandes, Lausanne, 1995.

[7] A. Bouscayrol, M. Pietrzak-David, P. Delarue, R. Peña-Eguiluz, P. E. Vidal, X. Kestelyn, "Weighted control of traction drives with parallel-connected AC machines", IEEE Trans. on Industrial Electronics, Vol.: 53, no 6, pp. 1799-1806, December 2006

[8] R. Peña-Eguiluz, M. Pietrzak-David and B. de Fornel, "Comparaison of several control strategies for parallel connected dual induction motors", International Conference on Power Electronics and Motion Control, EPE-PEMC'2002, Dubrovnik , Croatia

[9] W. Ben Mabrouk, J. Belhadj, I.Slama Belkodja, M.Pietrzak David “Analyse et modélisation de la charge mécanique d’une chaîne de traction ferroviaire à propulsion asynchrone” JTEA, pp 1548-1553, 02-04 Mai 2008, Hammamet, Tunisie
[10] C. Lochot, “Modélisation et caractérisation des phénomènes couplés dans une chaîne de traction ferroviaire asynchrone”, Thèse de Doctorat, INPT, Toulouse, 1999.
[11] S.Kadowaki, K.Ohishi, I.Miyashita, and S.Yasukawa “Anti-slip/skid Re-adhesion Control of Electric Motor Coach Based on Disturbance Observer and Sensor-less Vector Control”, EPE Journal, Vol.16, pp7-15, 2006
[12] Michael J.M.M. Steenbergen “Quantification of dynamic wheel–rail contact forces at short rail irregularities and application to measured rail welds” Journal of Sound and Vibration 312, pp 606–629, 2008.
[13] H. Chen, T. Ban, M. Ishid, T. Nakahara “Experimental investigation of influential factors on adhesion between wheel and rail under wet conditions” Wear 2008